Spatial Scheduling With Interference Cancellation in Multiuser MIMO Systems [1]

Yoshitaka Hara Loïc Brunel Kazuyoshi Oshima
Mitsubishi Electric Information Technology Centre Europe B.V. (ITE), France
1, allée de Beaulieu, CS 10806, 35708 Rennes Cedex 7, France

Abstract

This paper proposes a novel downlink spatial scheduling algorithm in multiuser MIMO systems, which selects good combination of terminals and base station(BS)'s transmit beams so that the BS's beams nullify inter-stream interference at the selected terminals. In the derivation process, we reveal new property that the optimization problem of downlink spatial scheduling is equivalent to that of uplink scheduling under the BS's zero-forcing beamforming. Using this property, an efficient downlink scheduling algorithm is presented applying principle of uplink scheduling algorithm. Numerical results show that the presented spatial scheduling achieves much higher system throughput than a multiuser MIMO system without spatial scheduling or with conventional spatial scheduling by linear processing. We also present a realistic control structure to achieve uplink and downlink spatial scheduling in time-division duplex (TDD) systems.

Index Terms

Mobile communications, MIMO systems, Scheduling, Beams, Traffic control

I. Introduction

Multi-input multi-output (MIMO) systems, which have multiple antennas at both transmitter and receiver, have been widely investigated for higher data rate wireless communications [1][2]. In future wireless communications, a multiuser MIMO system is expected to support multiple terminals accessing one base station (BS). Then, it is required to optimize the system considering many aspects of radio resource control, transmit beamforming, and modulation and coding scheme (MCS) [3]–[9].

So far, in multiuser MIMO systems, many papers have investigated efficient transmit or receive beamforming for signal transmission, assuming a fixed number of signals for each terminal [3]–[9]. In future multiuser MIMO systems, spatial scheduling would be also essential to improve system performance [10]–[17]. In spatial scheduling, terminals with good channel conditions are selected to send or receive signals

[1]This paper was presented in part at PIMRC'06, Helsinki, Finland, Sept. 2006 [29][30].

among possible terminals in each subband and in each time frame. The selected terminals send signals based on space division multiple access (SDMA) on uplink or receive signals based on space division multiplexing (SDM) on downlink. Selecting appropriate terminals, the spatial scheduling is expected to achieve higher spectrum efficiency than the system without spatial scheduling.

The SDM(A) transmission performance depends not only on signals' propagation gains but also on spatial correlation of the multiplexed signals. Since transmission performance deteriorates in case of high spatial correlation at the BS, it is required to select terminals and transmit beams for signal transmission, so that the multiplexed signals have low spatial correlation. Thus, the spatial scheduler is required to optimize combination of terminals and transmit beams under complex characteristics of SDM(A) transmission.

The optimum solution to this problem would be obtained by examining all possible combinations of terminals and transmit beams, but it requires huge and unrealistic complexity. Up to now, for uplink scheduling, appropriate combination of terminals has been sought by grouping terminals based on spatial correlation [11] or successive selection of terminals and their transmit beams [12]. Then, BS can suppress inter-stream interference using zero-forcing or minimum mean-squared error (MMSE) receive beamforming.

Meanwhile, on downlink, opportunistic random beamforming has been investigated [14][15], in which a terminal measures channel quality of random transmit beams and requests suitable one. Although this approach has small feedback of channel quality indicator, inter-stream interference remains at terminals. Downlink spatial scheduling with interference cancellation has been also investigated for terminals with single antenna [16] or multiple antennas [17]. In [17], spatial scheduler successively selects terminal and the BS's transmit beam to find an appropriate combination of terminals and the BS's transmit beams. In the successive selection, one difficulty lies in nullifying interference among multiplexed signals by linear processing, because already selected transmit beams interfere on the newly added signals. In [17], this problem has been solved by non-linear or Tomlinson-Harashima precoding [18][19], in which known interference from already selected signals can be neutralized by encoding the newly added signal. However, the solution of interference cancellation by linear processing only has not been known yet for downlink spatial scheduling under an arbitrary number of antennas at BS and terminals. To our best knowledge, [9] gives a local solution to this problem under a specific condition of multiuser MIMO without spatial scheduling. However, it is still an issue how the BS selects terminals and the BS's transmit beams nullifying inter-stream interference without examining all possible combinations in spatial scheduling. Furthermore, uplink and downlink spatial scheduling has been discussed separately and relationship of uplink and

downlink spatial scheduling in principle and performance has not been clarified yet.

In this paper, we first discuss natural extension of existing uplink scheduling to find an efficient uplink scheduling algorithm. Next, we propose a novel downlink scheduling algorithm which cancels inter-stream interference by linear processing only. The proposed downlink scheduling algorithm determines an appropriate combination of terminals and BS's transmit beams, so that each terminal can receive packet of interest without interference from the other multiplexed packets. In the derivation process, we reveal new property that the optimization problem of downlink spatial scheduling is equivalent to that of uplink spatial scheduling under the BS's zero-forcing beamforming. Using this property, we show that efficient downlink spatial scheduling can be performed applying principle of uplink scheduling algorithm. This property is also beneficial from implementation point of view, because uplink and downlink schedulers can be implemented as a common basic algorithm in a chipset. Moreover, we clarify that uplink and downlink spatial scheduling has similar performance based on the new property.

In [20][21], optimization of downlink transmit beamforming and transmit power control has been investigated applying uplink optimization algorithm under terminals with single antenna. Our research is different from [20][21] in selecting terminals with multiple antennas considering effect of the terminals' beams under no transmit power control. This paper presents equivalence of optimization problem in uplink and downlink spatial scheduling, but optimum algorithm has not been theoretically given yet. Nevertheless, the proposed algorithm provides efficient sub-optimum scheduling.

Furthermore, this paper presents a basic structure to control uplink and downlink spatial scheduling in time-division duplex (TDD) systems. Since it is essential to keep practical amount of control signalling for spatial scheduling, we present a realistic control structure, in which selected terminals can fulfill spatial scheduling according to the BS's instruction. The presented structure is novel in SDM-based control signalling towards selected terminals in multiuser MIMO systems, which have not been dealt with in previous investigation and standardization activities.

This paper is organized as follows. In section II, system model and basic control structure of spatial scheduling in multiuser MIMO systems are presented. In section III, natural extension of existing uplink spatial scheduling algorithm is discussed and, in section IV, a novel downlink spatial scheduling algorithm is proposed. In section V, performance of the proposed scheduling algorithm is evaluated and section VI gives the conclusion.

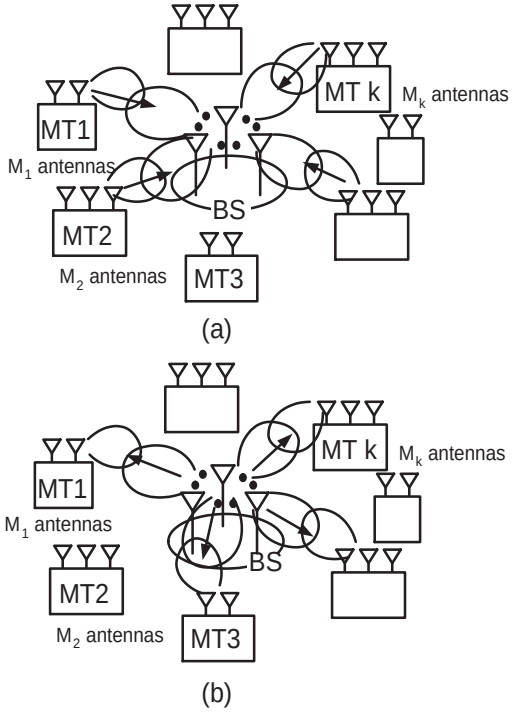

Fig. 1. Image of spatial scheduling in multiuser MIMO systems (a) uplink (b) downlink.

II. System Model and Basic Control Structure

Throughout the paper, we define the transpose as ^{T}, the complex conjugate as *, the complex conjugate transpose as †, the norm as $||\cdot||$, and the trace as tr$\{\cdot\}$.

In order to realize uplink and downlink spatial scheduling, not only scheduling algorithm but also control structure to fulfill spatial scheduling is essential. In this section, we describe system model and novel control structure to fulfill spatial scheduling supposing TDD systems.

A. MIMO Channel on Uplink

Let us consider a multiuser MIMO system which is composed of a BS with N antennas and K terminals, where the k-th terminal has M_k antennas ($k = 1, ..., K$). Fig. 1 (a) shows the image of uplink spatial scheduling in multiuser MIMO systems. The BS can receive at most N packets or signals simultaneously on uplink. The BS determines a terminal $k = k(n)$ and his transmit beamforming weight $M_{k(n)} \times 1$ vector $\hat{\boldsymbol{v}}_n$ ($||\hat{\boldsymbol{v}}_n|| = 1$) to send the n-th signal ($n = 1, ..., N$).

The BS informs the $k(n)$-th terminal of the transmit weight $\hat{\boldsymbol{v}}_n$ in advance and the terminal performs transmit beamforming based on the weight $\hat{\boldsymbol{v}}_n$. Assuming that the $k(n)$-th terminal transmits the n-th signal $\hat{s}_n(p)$ ($E[|\hat{s}_n(p)|^2] = 1$) with a constant power P_{UL}, the $N \times 1$ received signal vector $\boldsymbol{x}_{BS}(p)$

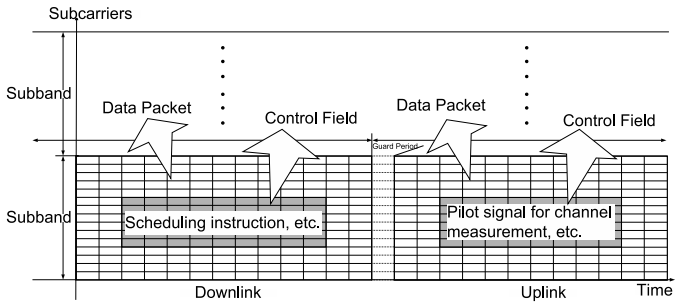

Fig. 2. Downlink and uplink frame formats for spatial scheduling in OFDMA/TDD/MIMO systems.

corresponding to the p-th sample at the BS is given by

$$\boldsymbol{x}_{BS}(p) = \sum_{n=1}^{n_{UL}} \sqrt{P_{UL}} \boldsymbol{H}_{k(n)}^{T} \hat{\boldsymbol{v}}_n \hat{s}_n(p) + \boldsymbol{z}_{BS}(p) \tag{1}$$

where $n_{UL}(\leq N)$ is the number of spatially multiplexed signals, $\boldsymbol{z}_{BS}(p)$ is the $N \times 1$ noise vector at the BS with $E[\boldsymbol{z}_{BS}(p)\boldsymbol{z}_{BS}^{\dagger}(p)] = P_{BS,z}\boldsymbol{I}$. The matrix $\boldsymbol{H}_k$ is the $M_k \times N$ channel matrix, where the (m,n)-th element of $\boldsymbol{H}_k$ represents the complex propagation gain from the BS's n-th antenna to the k-th terminal's m-th antenna. In this paper, we consider spatial scheduling for low-mobility terminals in TDD systems, where channel response is reciprocal between uplink and downlink [22][23]. The channel is assumed as quasi-stationary flat fading, which is a typical environment for a low-mobility terminal using a small subband of block subcarriers less than coherent bandwidth of multipath channels in orthogonal frequency division multiple access (OFDMA) systems [24][25]. The BS receives the n-th signal using $N \times 1$ beamforming weight vector $\hat{\boldsymbol{w}}_n$ and obtains the output $\hat{\boldsymbol{w}}_n^{T}\boldsymbol{x}_{BS}(p)$ ($n = 1, ..., n_{UL}$).

Assume that the BS has knowledge of the channel matrix $\boldsymbol{H}_k$ ($k = 1, ..., K$) and the noise power $P_{BS,z}$. In TDD systems, the channel matrix $\boldsymbol{H}_k$ is usually obtained by measuring responses through pilot signals from the k-th terminal's antennas on uplink. More exactly, the k-th terminal transmits M_k pilot signals from individual antennas, which could be practical amount of signalling. The noise power $P_{BS,z}$ is obtained by averaging $\boldsymbol{z}_{BS}^{\dagger}(p)\boldsymbol{z}_{BS}(p)/N$ over many samples. Using knowledge of $\boldsymbol{H}_k$ and $P_{BS,z}$, the BS determines the terminal $k(n)$, his transmit beamforming weight $\hat{\boldsymbol{v}}_n$, and the corresponding MCS to send the n-th signal. We refer to this transmission control scheme as uplink spatial scheduling.

B. Basic Control Structure of Uplink Spatial Scheduling

We present a novel control structure of uplink spatial scheduling, supposing OFDMA/TDD/MIMO systems as a practical example. Fig. 2 shows the downlink and uplink frame formats to achieve uplink spatial scheduling in OFDMA/TDD/MIMO systems. On downlink, scheduling instruction is sent in control

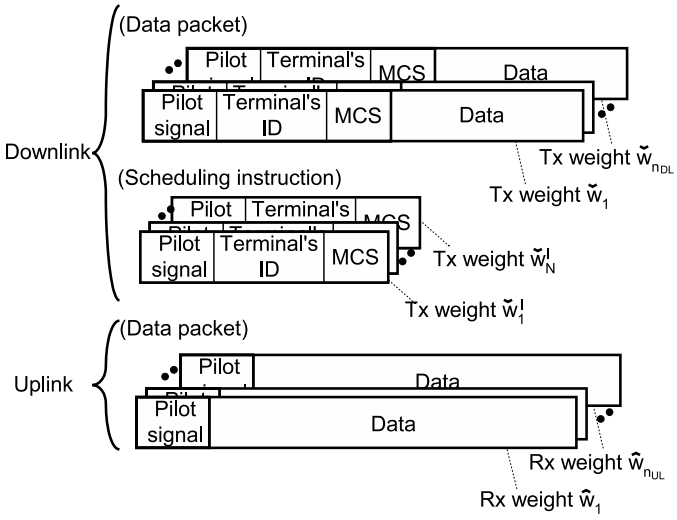

Fig. 3. Packet and scheduling instruction formats (a) uplink (b) downlink.

field on subband basis, in which the BS reports the terminal number $k(n)$, the transmit weight $\hat{\boldsymbol{v}}_n$, and the corresponding MCS information $(n = 1, ..., n_{UL})$ determined by scheduling algorithm to terminals.

Fig. 3 shows the packet and scheduling instruction formats. In the downlink control field, N different instructions are spatially multiplexed by different transmit beams based on the $N \times 1$ weight vectors $\check{\boldsymbol{w}}^I_1$, ..., $\check{\boldsymbol{w}}^I_N$. One instruction contains pilot signal of fixed pattern, terminal's identifier (ID), and MCS information, where the pilot signals are mutually orthogonal in different instructions [1]. The weights $\check{\boldsymbol{w}}^I_1, ..., \check{\boldsymbol{w}}^I_N$ are given by

$$\begin{aligned} [\check{\boldsymbol{w}}^I_1, ..., \check{\boldsymbol{w}}^I_N] &= N^{1/2} \frac{(\boldsymbol{B}^*_{norm} \boldsymbol{B}^T_{norm})^{-1} \boldsymbol{B}^*_{norm}}{\mathrm{tr}\{(\boldsymbol{B}^*_{norm} \boldsymbol{B}^T_{norm})^{-1}\}^{1/2}} \\ \boldsymbol{B}_{norm} &= [\boldsymbol{b}_1/||\boldsymbol{b}_1||, ..., \boldsymbol{b}_N/||\boldsymbol{b}_N||] \end{aligned} \tag{2}$$

where $\boldsymbol{b}_n = \sqrt{P_{UL}} \boldsymbol{H}^T_{k(n)} \hat{\boldsymbol{v}}_n (n = 1, ..., n_{UL})$ and $\boldsymbol{b}_n (n = n_{UL} + 1, ..., N)$ is successively selected to be orthogonal to $\boldsymbol{b}_1$, ..., $\boldsymbol{b}_{n-1}$. Under (2), the $k(n)$-th terminal can compute the target transmit weight $\hat{\boldsymbol{v}}_n$ using responses of the N pilot signals in the N instructions [26].

When the instructions arrive at a terminal, the terminal performs receive beamforming for each instruction, using the fixed pilot signal as reference signal. At output of receive beamformer, the terminal checks terminal ID in each instruction. If the terminal ID corresponds to the terminal's one, the terminal recognizes the instruction to send a packet on the next uplink frame, otherwise the terminal skips the instruction. The terminal obtains the instruction number n of recognition from the fixed pilot pattern and

[1]The N instructions are always sent on downlink. In case of $n_{UL} < N$, terminal ID and MCS information in the $n_{UL} + 1, ..., N$-th instructions indicate blank information.

reads MCS information. Moreover, the terminal computes the $M_{k(n)} \times 1$ target weight $\hat{\boldsymbol{v}}_n$ from responses of the N pilot signals in the N instructions [26].

The $k(n)$-th terminal sends the n-th packet using the instructed MCS and the transmit beamforming weight $\hat{\boldsymbol{v}}_n$ based on SDMA ($n = 1, ..., n_{UL}$), where each packet contains pilot and data signals as shown in Fig. 3. The pilot pattern of the n-th packet is fixed and orthogonal to those of the other packets. The BS performs beamforming to receive the n-th uplink packet using the n-th fixed pilot signal as reference signal ($n = 1, ..., n_{UL}$). Even though the uplink packet does not include terminal's ID and MCS information, the BS can identify the terminal ID and MCS information by checking the n-th pilot pattern of uplink packet and referring the n-th scheduling instruction information stored at the BS.

Based on the above basic control structure, terminals can recognize and fulfill uplink scheduling instructions. On downlink, the selected $k(n)$-th terminal can receive the n-th instruction with good channel quality (see appendix I). Although the other terminals may miss the n-th instruction, it does not cause any problem if they detect error and skip the n-th instruction. So far, SDM-based control signalling has not been considered in multiuser MIMO systems, because conventional signalling is designed such that all terminals receive it correctly. However, allowing the terminals $k \neq k(n)$ to skip the n-th instruction, the presented structure conveys multiple instructions efficiently based on SDM. Moreover, the pilot signals in the N instructions are used efficiently for both purposes of receiving instructions and computing the transmit weight $\hat{\boldsymbol{v}}_n$.

In uplink spatial scheduling, the terminal ID, the transmit weight, and MCS will change in different subbands and in different time frames. The terminal can fulfill the BS's system control checking instructions in each subband and in each time frame. Since spectrum efficiency depends on strategy to determine the terminal ID, the transmit weight, and MCS, we discuss an efficient uplink scheduling algorithm in section III.

C. MIMO Channel on Downlink

Next, we consider downlink spatial scheduling under a BS with N antennas and K terminals. Although we use the same notation of terminals $k = 1, ..., K$ as in uplink scheduling for simple explanation, the downlink scheduling is applicable to different possible terminals from those for uplink scheduling. Fig. 1 (b) shows the image of downlink spatial scheduling in multiuser MIMO systems.

The BS transmits $n_{DL}(\leq N)$ packets or signals, simultaneously, using different transmit beams based on the $N \times 1$ weights $\check{\boldsymbol{w}}_n$ ($||\check{\boldsymbol{w}}_n|| = 1$, $n = 1, ..., n_{DL}$). Assuming that the n-th signal $\check{s}_n(p)$ ($E[|\check{s}_n(p)|^2] = 1$)

is transmitted from the n-th transmit beam with a constant power P_{DL}, the k-th terminal receives the $M_k \times 1$ signal vector $\boldsymbol{x}_k(p)$ corresponding to the p-th sample as

$$\boldsymbol{x}_k(p) = \sum_{n=1}^{n_{DL}} \sqrt{P_{DL}} \boldsymbol{H}_k \check{\boldsymbol{w}}_n \check{s}_n(p) + \boldsymbol{z}_k(p) \quad (3)$$

where $\boldsymbol{z}_k(p)$ is the $M_k \times 1$ noise vector at the k-th terminal with $E[\boldsymbol{z}_k(p)\boldsymbol{z}_k(p)^\dagger] = P_{kz}\boldsymbol{I}$ and P_{kz} is the k-th terminal's noise power. The k-th terminal performs beamforming to receive the signal based on the $M_k \times 1$ weight $\check{\boldsymbol{v}}_k$ and obtains the output $\check{\boldsymbol{v}}_k^T \boldsymbol{x}_k(p)$.

We assume that the BS has knowledge of the channel matrix $\boldsymbol{H}_k$ and the noise power P_{kz} ($k = 1, ..., K$). The noise power P_{kz} is reported from the k-th terminal on uplink. Using knowledge of $\boldsymbol{H}_k$ and P_{kz}, the BS determines the terminal $k(n)$ to which the n-th packet is sent, the transmit weight $\check{\boldsymbol{w}}_n$ for the n-th packet, and the corresponding MCS in each subband and in each time frame. We refer to this transmission control scheme as downlink spatial scheduling.

D. Basic Control Structure for Downlink Spatial Scheduling

As shown in Fig. 3, a downlink packet includes pilot signal, terminal's identifier (ID), MCS information, and encoded data symbols based on the MCS. Although the n-th transmit weight $\check{\boldsymbol{w}}_n$ changes in different subbands and in different time frames, the n-th downlink packet always includes the n-th fixed pilot pattern which is orthogonal to those in the other multiplexed packets.

Similarly to II-B, each terminal performs receive beamforming using the n-th fixed pilot pattern and checks the terminal ID at the output of the beamformer. If the terminal ID corresponds to the terminal's one, the terminal receives data symbols based on the MCS information. Terminals can find packets of interest, checking the terminal ID in each subband and in each time frame. Since spectrum efficiency greatly depends on strategy to determine the terminal ID, the transmit weight, and MCS, we study an efficient downlink scheduling algorithm in section IV. The uplink and downlink spatial scheduling is performed independently to deal with asymmetric communications.

III. Uplink Spatial Scheduling Algorithm

In this section, we discuss uplink spatial scheduling algorithm [12] and its natural extension. It is important to know efficient uplink scheduling algorithm, because it affects downlink scheduling algorithm as explained later in IV.

A. Characteristics of Received Signal

Consider that the $k(1), ..., k(n)$-th terminals send the $1, ..., n$-th uplink packets, respectively. Then, the received signal at the BS is expressed as

$$\boldsymbol{x}_{BS}(p) = \sum_{l=1}^{n} \sqrt{P_{UL}} \boldsymbol{H}_{k(l)}^{T} \hat{\boldsymbol{v}}_l \hat{s}_l(p) + \boldsymbol{z}_{BS}(p) \tag{4}$$

where the signals $\hat{s}_{l_1}(p)$ and $\hat{s}_{l_2}(p)$ from different terminals $l_1 \neq l_2$ are statistically independent. Consider that the BS receives the l-th signal $\hat{s}_l(p)$ using beamforming based on the weight $\hat{\boldsymbol{w}}_l$. Then, the signal-to-interference-plus-noise ratio (SINR) of the l-th signal at output of beamformer, which maximizes the output SINR using $\hat{\boldsymbol{w}}_l = (\boldsymbol{\Phi}_{l|n}^{-1} \boldsymbol{H}_{k(l)}^{T} \hat{\boldsymbol{v}}_l)^*$, is given by [5]

$$\hat{\gamma}_{l|n} = P_{UL} \hat{\boldsymbol{v}}_l^{\dagger} \boldsymbol{H}_{k(l)}^{*} \boldsymbol{\Phi}_{l|n}^{-1} \boldsymbol{H}_{k(l)}^{T} \hat{\boldsymbol{v}}_l \tag{5}$$

$$\boldsymbol{\Phi}_{l|n} = \sum_{i=1, i\neq l}^{n} P_{UL} \boldsymbol{H}_{k(i)}^{T} \hat{\boldsymbol{v}}_i \hat{\boldsymbol{v}}_i^{\dagger} \boldsymbol{H}_{k(i)}^{*} + P_{BS,z} \boldsymbol{I}. \tag{6}$$

Furthermore, under fixed $\hat{\boldsymbol{v}}_1, ..., \hat{\boldsymbol{v}}_{l-1}, \hat{\boldsymbol{v}}_{l+1}, ..., \hat{\boldsymbol{v}}_n$, the SINR $\hat{\gamma}_{l|n}$ is maximized to $P_{UL}\ \rho\langle\ \boldsymbol{H}_{k(l)}^{*}\ \boldsymbol{\Phi}_{l|n}^{-1}\ \boldsymbol{H}_{k(l)}^{T}\rangle$ by using $\hat{\boldsymbol{v}}_l = \boldsymbol{e}\langle \boldsymbol{H}_{k(l)}^{*} \boldsymbol{\Phi}_{l|n}^{-1} \boldsymbol{H}_{k(l)}^{T}\rangle$, where $\rho\langle \boldsymbol{A}\rangle$ and $\boldsymbol{e}\langle \boldsymbol{A}\rangle$ are the maximum eigenvalue and the corresponding eigenvector of the matrix $\boldsymbol{A}$, respectively.

B. Uplink Spatial Scheduling Algorithm

As natural extension of [12], we describe uplink spatial scheduling algorithm which selects terminals to achieve largest output SINR successively in the presence of determined signals as follows :

[Uplink Spatial Scheduling Algorithm]

1) Initialize $n = 1$ and $F_{UL}(0) = 0$.
2) Compute $\rho_k = \rho\langle \boldsymbol{H}_k^{*} \boldsymbol{\Phi}_{n|n}^{-1} \boldsymbol{H}_k^{T}\rangle$ for all terminals $k = 1, ..., K$ and select the terminal k which has largest ρ_k as the terminal $k(n)$. Decide the $k(n)$-th terminal's transmit weight as $\hat{\boldsymbol{v}}_n = \boldsymbol{e}\langle \boldsymbol{H}_{k(n)}^{*}\ \boldsymbol{\Phi}_{n|n}^{-1}\ \boldsymbol{H}_{k(n)}^{T}\rangle$. [2]
3) Compute system throughput $F_{UL}(n)$ in the presence of n determined signals. If $F_{UL}(n) > F_{UL}(n-1)$, go to 4), otherwise $n_{UL} = n - 1$ and end.

[2]The algorithm examines ρ_k of all terminals including $k = k(1), ..., k(n-1)$ for the n-th signal. It is also possible to exclude $k = k(1), ..., k(n-1)$ as an alternative way, in which the BS has slightly less complexity and lower system performance due to lost opportunity of selecting terminals $k = k(1), ..., k(n-1)$ twice. Actually, probability of selecting the terminals $k = k(1), ..., k(n-1)$ twice is very small in case of $K \geq N$ under similar statistical characteristics of $\boldsymbol{H}_k$ for all k, because the terminals $k = k(1), ..., k(n-1)$ have penalty of interference from their previously determined signals. However, the presented algorithm improves system performance in case of $K < N$, allowing one terminal to use multiple eigenmodes. Whether to include or exclude $k = k(1), ..., k(n-1)$ for the n-th signal depends on design policy.

4) If $n < N$, increase n by 1 and go back to 2), otherwise $n_{UL} = n$ and end.

In step 3), the system throughput is computed as $F_{UL}(n) = \sum_{l=1}^{n} f_{UL}(\hat{\gamma}_{l|n})$, where $f_{UL}(\cdot)$ is the throughput of one packet. The throughput $f_{UL}(\gamma)$ is a function of SINR γ and prepared in advance as look-up table. After the above algorithm, the scheduler computes the SINR $\hat{\gamma}_{l|n_{UL}}$ and decides MCS for each packet, referring the predetermined look-up table of SINR to MCS.

Since the algorithm selects terminals and their transmit weights to maximize SINR successively, the scheduler is expected to achieve higher spectrum efficiency. In the scheduler, a newly added signal may degrade the previously determined signals. However, the newly added signal which achieves high SINR is likely to have low spatial correlation with the previously determined signals. In this case, the performance deterioration in the first to $(n-1)$-th signals will be small. If the n-th signal greatly degrades the previously determined signals, the scheduler rejects the n-th signal and keeps the system throughput in step 3). We refer to this algorithm as "maxSINR" algorithm.

C. Iterative Transmit Weight Computation

After the above scheduling procedure, we examine effect of the following iterative transmit weight (ITW) computation shown in [5] to refine weights $\hat{\boldsymbol{v}}_l$, because the SINR may be partially degraded by new signals.

[Iterative Transmit Weight (ITW) Computation]

1) Initialize $i = 1$.
2) Update the weight $\hat{\boldsymbol{v}}_l$ ($l = 1, ..., n_{UL}$) successively by

$$\boldsymbol{e}\langle \boldsymbol{H}^{*}_{k(l)} \boldsymbol{\Phi}^{-1}_{l|n_{UL}} \boldsymbol{H}^{T}_{k(l)} \rangle \rightarrow \hat{\boldsymbol{v}}_l \tag{7}$$

3) If $i < i_{max}$, increase i by 1 and go back to 2), otherwise end, where i_{max} is the maximum iteration number.

The MCS is determined after this algorithm. We refer to this algorithm as "ITW" algorithm. Although optimality of maxSINR or ITW algorithm has not been proven yet, these algorithms basically provide efficient transmission performance [5][13].

IV. Proposed Downlink Spatial Scheduling Algorithm

We propose novel downlink spatial scheduling algorithm based on zero-forcing transmit beamforming.

A. Zero-Forcing Transmit Beamforming

Consider that the BS sends the 1, ..., n-th packets to the $k(1)$, ..., $k(n)$-th terminals, respectively. Then, the received signal vector at the k-th terminal is expressed as

$$\boldsymbol{x}_k(p) = \sum_{l=1}^{n} \sqrt{P_{DL}} \boldsymbol{H}_k \check{\boldsymbol{w}}_l \check{s}_l(p) + \boldsymbol{z}_k(p) \tag{8}$$

It is essential to find efficient transmit weights $\check{\boldsymbol{w}}_1, ..., \check{\boldsymbol{w}}_n$ in spatial scheduling. We consider the zero-forcing transmit weights $\check{\boldsymbol{w}}_1, ..., \check{\boldsymbol{w}}_n$, which satisfy

$$\begin{aligned} \sqrt{P_{DL}} \cdot [\check{\boldsymbol{w}}_1, ..., \check{\boldsymbol{w}}_n] &= \boldsymbol{B}^*(\boldsymbol{B}^T\boldsymbol{B}^*)^{-1}\boldsymbol{P}'^{1/2} \\ \boldsymbol{B} &= [\boldsymbol{H}_{k(1)}^T \tilde{\boldsymbol{v}}_1, ..., \boldsymbol{H}_{k(n)}^T \tilde{\boldsymbol{v}}_n] \\ \boldsymbol{P}' &= \text{diag}[P_1', ..., P_n'] \end{aligned} \tag{9}$$

where the $M_{k(l)} \times 1$ vector $\tilde{\boldsymbol{v}}_l$ ($||\tilde{\boldsymbol{v}}_l|| = 1$) denotes the $k(l)$-th terminal's virtual weight to receive the l-th packet and P_l' ($l = 1, ..., n$) is the parameter to normalize $\check{\boldsymbol{w}}_l$ to $||\check{\boldsymbol{w}}_l|| = 1$. The virtual weight $\tilde{\boldsymbol{v}}_l$ is used only in the spatial scheduling algorithm.

From (9), we have $\boldsymbol{B}^T[\check{\boldsymbol{w}}_1, ..., \check{\boldsymbol{w}}_n] = \boldsymbol{P}'^{1/2}/P_{DL}^{1/2}$ and the (n, l)-th element of $\boldsymbol{B}^T[\check{\boldsymbol{w}}_1, ..., \check{\boldsymbol{w}}_n]$ is expressed as

$$(\boldsymbol{H}_{k(n)}^T \tilde{\boldsymbol{v}}_n)^T \check{\boldsymbol{w}}_l = \tilde{\boldsymbol{v}}_n^T (\boldsymbol{H}_{k(n)} \check{\boldsymbol{w}}_l) = \begin{cases} \sqrt{P_n'/P_{DL}} & l = n \\ 0 & l \neq n \end{cases} . \tag{10}$$

In the above equation, $\tilde{\boldsymbol{v}}_n^T(\boldsymbol{H}_{k(n)}\check{\boldsymbol{w}}_l)$ corresponds to the l-th signal's amplitude at output of the $k(n)$-th terminal's receive beamforming based on the weight $\tilde{\boldsymbol{v}}_n$. This means that the $k(n)$-th terminal can nullify interference from all multiplexed packets except the n-th packet, using the virtual weight $\tilde{\boldsymbol{v}}_n$. Likewise, each terminal can receive the packet of interest, nullifying interference from the other packets. Hence, a set of the transmit weights $\check{\boldsymbol{w}}_l$ and the virtual receive weights $\tilde{\boldsymbol{v}}_l$ in (9) is a solution of multiuser channel diagonalization [4], which nullifies interference from the other packets at each terminal. Since the multiuser channel diagonalization [4] holds for any vector $\tilde{\boldsymbol{v}}_l$, the transmit weights in (9) have degrees of freedom in deciding the virtual weight $\tilde{\boldsymbol{v}}_l$. The virtual weight $\tilde{\boldsymbol{v}}_l$ will be determined later by scheduling strategy of SINR maximization.

In some previous papers [3][7][8], transmit beamforming nullifies interference to active terminals' antennas except the desired terminal. Then, the number of multiplexed signals is restricted by the total number of active terminals' antennas. In contrast, the presented zero-forcing transmit beamforming nullifies

interference to active terminals' virtual beams based on the weight $\tilde{\boldsymbol{v}}_n$. Consequently, the presented transmit beamforming can multiplex N packets without inter-stream interference, whatever the number of active terminals' antennas is. The same property has been seen in [9] for a specific condition of multiuser MIMO without spatial scheduling. However, it is still problem how downlink scheduler selects terminals and transmit beams efficiently nullifying inter-stream interference without examining all possible combinations.

B. Terminal's Received SINR

Since the $k(l)$-th terminal has no interference from the other multiplexed packets, the $k(l)$-th terminal's received SINR $\check{\gamma}_{l|n}$ (equal to SNR, thanks to zero-forcing beamforming) in the presence of n packets is given by

$$\check{\gamma}_{l|n} = P_{DL}\frac{|\tilde{\boldsymbol{v}}_l^T \boldsymbol{H}_{k(l)}\check{\boldsymbol{w}}_l|^2}{P_{k(l)z}||\tilde{\boldsymbol{v}}_l||^2} = \frac{P_l^{'}}{P_{k(l)z}}. \tag{11}$$

Using the $n \times 1$ vector $\boldsymbol{d}_{l|n} = [0, ..., 0, 1, 0, ..., 0]^T$ which has 1 in the l-th element and 0 in the other elements, (9) gives

$$P_{DL} = P_{DL}\check{\boldsymbol{w}}_l^T\check{\boldsymbol{w}}_l^* = P_l^{'}\boldsymbol{d}_{l|n}^{\dagger}(\boldsymbol{B}^{\dagger}\boldsymbol{B})^{-1}\boldsymbol{d}_{l|n}. \tag{12}$$

Therefore, $\check{\gamma}_{l|n}$ is transformed into

$$\check{\gamma}_{l|n} = \frac{P_{DL}}{P_{k(l)z}\boldsymbol{d}_{l|n}^{\dagger}(\boldsymbol{B}^{\dagger}\boldsymbol{B})^{-1}\boldsymbol{d}_{l|n}}. \tag{13}$$

Using appendix II, the SINR in (13) is further transformed into

$$\begin{aligned}
\check{\gamma}_{l|n} &= \frac{P_{DL}}{P_{k(l)z}}\tilde{\boldsymbol{v}}_l^{\dagger}\boldsymbol{H}_{k(l)}^*\boldsymbol{\Psi}_{l|n}\boldsymbol{H}_{k(l)}^T\tilde{\boldsymbol{v}}_l \\
\boldsymbol{\Psi}_{l|n} &= \boldsymbol{I} - \bar{\boldsymbol{B}}_{l|n}(\bar{\boldsymbol{B}}_{l|n}^{\dagger}\bar{\boldsymbol{B}}_{l|n})^{-1}\bar{\boldsymbol{B}}_{l|n}^{\dagger} \\
\bar{\boldsymbol{B}}_{l|n} &= [\boldsymbol{H}_{k(1)}^T\tilde{\boldsymbol{v}}_1, ..., \boldsymbol{H}_{k(l-1)}^T\tilde{\boldsymbol{v}}_{l-1}, \\
&\qquad \boldsymbol{H}_{k(l+1)}^T\tilde{\boldsymbol{v}}_{l+1}, ..., \boldsymbol{H}_{k(n)}^T\tilde{\boldsymbol{v}}_n]
\end{aligned} \tag{14}$$

where the matrix $\bar{\boldsymbol{B}}_{l|n}$ is the $N \times (n-1)$ aggregation matrix of columns $\boldsymbol{H}_{k(l')}^T\tilde{\boldsymbol{v}}_{l'}$ $(l' = 1, ..., l-1, l+1, ..., n)$ except the column for the l-th signal. Since the matrix $\bar{\boldsymbol{B}}_{l|n}$ does not depend on $\tilde{\boldsymbol{v}}_l$, the SINR $\check{\gamma}_{l|n}$ is maximized to $\check{\gamma}_{l|n} = (P_{DL}/P_{k(l)z}) \cdot \rho\langle\boldsymbol{H}_{k(l)}^*\boldsymbol{\Psi}_{l|n}\boldsymbol{H}_{k(l)}^T\rangle$ by using $\tilde{\boldsymbol{v}}_l = \boldsymbol{e}\langle\boldsymbol{H}_{k(l)}^*\boldsymbol{\Psi}_{l|n}\boldsymbol{H}_{k(l)}^T\rangle$, under fixed $\tilde{\boldsymbol{v}}_1, ..., \tilde{\boldsymbol{v}}_{l-1}, \tilde{\boldsymbol{v}}_{l+1}, ..., \tilde{\boldsymbol{v}}_n$.

The SINR (14) is obtained at the $k(l)$-th terminal using the virtual receive weight $\tilde{\boldsymbol{v}}_l$. In our study, downlink spatial scheduling algorithm assumes this interference cancellation state as baseline. Correspondingly,

we attempt to find an efficient spatial scheduling algorithm with interference cancellation to improve the baseline performance.

It is another issue how the $k(l)$-th terminal gets the weight $\tilde{\boldsymbol{v}}_l$ in practice without downlink control information. In some conditions, the $k(l)$-th terminal could likely get the weight $\tilde{\boldsymbol{v}}_l$ by zero-forcing weight which nullifies the $l^{'}$-th packet $(l^{'} = 1, ..., l-1, l+1, ..., n)$ according to relationship of $\tilde{\boldsymbol{v}}_l^T(\boldsymbol{H}_{k(l)}\check{\boldsymbol{w}}_{l'}) = 0$ in (10). Another practical way is that the $k(l)$-th terminal uses the MMSE weight instead of $\tilde{\boldsymbol{v}}_l$, where the MMSE weight maximizes output SINR of the l-th packet. Since the MMSE weight achieves higher output SINR than the virtual weight $\tilde{\boldsymbol{v}}_l$, the SINR (14) is guaranteed under the MMSE weight. Thus, it is possible in practice to keep the baseline performance at terminals.

C. Downlink Spatial Scheduling Algorithm

The SINR formula in (14) has similar expression to (5) of uplink spatial scheduling. Consider virtual uplink that the $k(l)$-th terminal transmits the l-th signal using transmit beamforming weight $\tilde{\boldsymbol{v}}_l$ with the power $P_{DL}/P_{k(l)z}$. Then, the SINR of (14) is identical to output SINR of the BS's zero-forcing receive beamformer in the presence of unit noise power. Therefore, the optimization problem of downlink spatial scheduling is equivalent to that of the virtual uplink spatial scheduling.

In section III, we have discussed an efficient uplink spatial scheduling algorithm, in which terminals and the terminals' transmit beams are successively determined. Considering equivalence between downlink and virtual uplink scheduling, the same strategy will be applied to downlink spatial scheduler. Accordingly, we present a novel downlink scheduling algorithm which determines terminal $k(n)$, transmit weight $\check{\boldsymbol{w}}_n$, and MCS for the n-th packet ($n = 1, ..., n_{DL}$) as follows :

[Downlink Spatial Scheduling Algorithm]

1) Initialize $n = 1$ and $F_{DL}(0) = 0$.
2) Compute $\rho_k = \rho\langle \boldsymbol{H}_k^* \boldsymbol{\Psi}_{n|n} \boldsymbol{H}_k^T \rangle$ for all terminals $k = 1, ..., K$ and select the terminal k which has largest SINR $(P_{DL}/P_{kz})\rho_k$ as the terminal $k(n)$. Decide the $k(n)$-th terminal's virtual weight as $\tilde{\boldsymbol{v}}_n = \boldsymbol{e}\langle \boldsymbol{H}_{k(n)}^* \boldsymbol{\Psi}_{n|n} \boldsymbol{H}_{k(n)}^T \rangle$.
3) Compute system throughput $F_{DL}(n)$ in the presence of the determined n signals. If $F_{DL}(n) > F_{DL}(n-1)$, go to 4), otherwise $n_{DL} = n - 1$ and go to 5).
4) If $n < N$, increase n by 1 and go back to 2), otherwise $n_{DL} = n$ and go to 5).
5) Compute $P_1^{'}, ..., P_{n_{DL}}^{'}$ using (12) and the transmit weights $\check{\boldsymbol{w}}_1, ..., \check{\boldsymbol{w}}_{n_{DL}}$ using (9), and end.

After the above algorithm, the scheduler computes the SINR $\check{\gamma}_{l|n_{DL}}$ and decides MCS for each packet, using the look-up table of SINR to MCS. In step 3), the system throughput $F_{DL}(n)$ is given by $F_{DL}(n) = \sum_{l=1}^{n} f_{DL}(\check{\gamma}_{l|n})$, where $f_{DL}(\cdot)$ is the throughput function for downlink.

In this algorithm, the virtual weights $\tilde{\boldsymbol{v}}_n$ are successively decided and the transmit weights $\check{\boldsymbol{w}}_1, ..., \check{\boldsymbol{w}}_n$ are fixed after determination of all packets. Note that [17] decides the transmit weights $\check{\boldsymbol{w}}_1, ..., \check{\boldsymbol{w}}_n$ successively, in which previously determined transmit beamformers give interference to the newly added signals. Our scheduler solves the problem of inter-stream interference nullification and the transmit weights $\check{\boldsymbol{w}}_1, ..., \check{\boldsymbol{w}}_n$ nullify interference to the selected terminals' virtual receive beams except the desired terminal's one. On the other hand, the terminal's received signal power in our scheduler may be lower than in [17]. Similarly to uplink spatial scheduler, the presented downlink scheduler is expected to achieve high system throughput.

D. Iterative Virtual Weight Computation

After the above scheduling procedure, we examine effect of the following iterative virtual weight (IVW) computation.

[Iterative Virtual Weight (IVW) Computation]

1) Initialize $i = 1$.
2) Update the weight $\tilde{\boldsymbol{v}}_l$ ($l = 1, ..., n_{DL}$) successively by

$$\boldsymbol{e}\langle \boldsymbol{H}^{*}_{k(l)} \boldsymbol{\Psi}_{l|n_{DL}} \boldsymbol{H}^{T}_{k(l)} \rangle \rightarrow \tilde{\boldsymbol{v}}_l \tag{15}$$

3) If $i < i_{max}$, increase i by 1 and go back to 2), otherwise compute $P^{'}_{1}, ..., P^{'}_{n_{DL}}$ using (12) and the transmit weights $\check{\boldsymbol{w}}_1, ..., \check{\boldsymbol{w}}_{n_{DL}}$ using (9), and end.

The MCS is determined after this algorithm. The iterative virtual weight computation is turned out equivalent to algorithm [9] (see appendix III), which gives a local solution of interference nullification under multiuser MIMO without spatial scheduling.

E. Discussions

The proposed downlink scheduling algorithm will give a solution to the problem how to select terminals and transmit beams nullifying inter-stream interference on downlink. According to the new property of equivalence between uplink and downlink schedulers, future development of uplink scheduler in performance, complexity, fairness, etc., straightforwardly improves downlink scheduler. In this sense, more importantly, this paper presents not only a specific downlink scheduling algorithm in IV-C, but

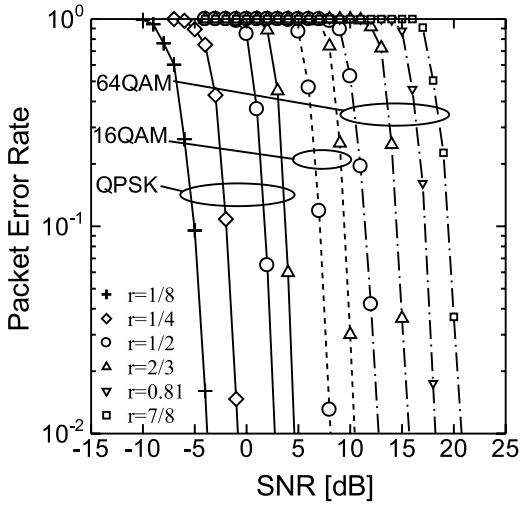

Fig. 4. Packet error rate under various MCSs.

TABLE I

SELECTION OF MCS BASED ON RECEIVED SINR AND THE CORRESPONDING THROUGHPUT (TP).

SINR [dB]	Modulation	Coding Rate	TP [b/s/Hz]
$\sim$ -5.0	No use	—-	0
-5.0 $\sim$ -1.9	QPSK	1/8	0.25
-1.9 $\sim$ 1.8	QPSK	1/4	0.50
1.8 $\sim$ 3.8	QPSK	1/2	1.00
3.8 $\sim$ 7.1	QPSK	2/3	1.33
7.1 $\sim$ 9.3	16QAM	1/2	2.00
9.3 $\sim$ 11.3	16QAM	2/3	2.67
11.3 $\sim$ 14.5	64QAM	1/2	3.00
14.5 $\sim$ 17.2	64QAM	2/3	4.00
17.2 $\sim$ 19.5	64QAM	0.81	4.86
19.5 $\sim$	64QAM	7/8	5.25

also indicates wide application of uplink scheduling algorithm explored in future research. This is also beneficial from implementation viewpoint, because uplink and downlink scheduling algorithms can be implemented as a common algorithm in a chipset. Using the new property, we can intuitively understand that uplink and downlink spatial scheduling has similar performance.

In papers [20][21], optimization of downlink transmit beamforming based on virtual uplink concept has been considered for single antenna at terminals under transmit power control. The proposed algorithm is different from [20][21] in selecting appropriate terminals with multiple antennas under no transmit power control, considering effect of the terminals' receive beamforming.

V. PERFORMANCE EVALUATION

The proposed spatial schedulers are evaluated by simulations.

A. Simulation Parameters

In computer simulations, we consider isolated cell environment of one BS with $N = 4$ antennas and K terminals, where all the terminals have the same number of antennas $M_k = M$. The terminals have the MIMO channel matrix $\boldsymbol{H}_k$, the elements of which are independent identically distributed (i.i.d.) complex Gaussian random variables with zero mean and unit variance. The BS has white noise with the power $P_{BS,z}$ per antenna. All terminals are assumed to have the same noise power $P_{kz} = P_z$ per antenna.

Each of uplink packet and downlink packet contains 150 convolutionally encoded data symbols based on the instructed MCS. Fig. 4 shows the packet error rate (PER) versus E_b/N_0 for various types of MCSs in single-input single-output (SISO)-additive white Gaussian noise (AWGN) channel. The BS selects MCS based on the SINR, $\hat{\gamma}_{n|n_{UL}}$ or $\check{\gamma}_{n|n_{DL}}$, for each packet which maximizes throughput under the constraint of PER $\leq 10^{-1}$. Table I lists the appropriate MCS to meet PER $\leq 10^{-1}$ and the corresponding throughput for various SINRs. The throughput function $f_{UL}(\gamma)(= f_{DL}(\gamma))$ is determined by Table I.

For comparison purpose, we evaluate the case without spatial scheduling, where constant four terminals send (receive) one packet individually on uplink (downlink). On uplink, the $k(n)$-th terminal $(k(n) = n = 1, ..., 4)$ sends the n-th signal using transmit weight $\hat{\boldsymbol{v}}_n^{(0)}$, where $\hat{\boldsymbol{v}}_n^{(0)}$ is given by eigenbeamforming, i. e. $\hat{\boldsymbol{v}}_n^{(0)} = \boldsymbol{e}\langle \boldsymbol{H}_{k(n)}^* \boldsymbol{H}_{k(n)}^T \rangle$, without iterative transmit weight computation or $\hat{\boldsymbol{v}}_n^{(0)}$ is updated i_{max} times by (7) with iterative transmit weight computation. MCS of each packet is determined from the computed SINR. Likewise, on downlink, the BS computes the transmit weight $\check{\boldsymbol{w}}_n$ based on the virtual weight $\tilde{\boldsymbol{v}}_n^{(0)}$, where $\tilde{\boldsymbol{v}}_n^{(0)}$ is given by $\tilde{\boldsymbol{v}}_n^{(0)} = \boldsymbol{e}\langle \boldsymbol{H}_{k(n)}^* \boldsymbol{H}_{k(n)}^T \rangle$ without iterative virtual weight computation or $\tilde{\boldsymbol{v}}_n^{(0)}$ is updated i_{max} times by (15) with iterative virtual weight computation.

B. System Throughput of Uplink Spatial Scheduling

We examine system throughput of uplink scheduling algorithm to find an efficient scheduling algorithm. Fig. 5 shows the system throughput of uplink spatial scheduling based on maxSINR+ITW algorithm along with that of no spatial scheduling with ITW algorithm under $P_{UL}/P_{BS,z} = 10$ dB. In the figure, the system throughput is enhanced by spatial scheduling, as the number of terminals K increases, because the selected uplink signals have better channel quality and lower spatial correlation at the BS. In case of no spatial scheduling, the fixed four terminals always send one packet, whereas spatial scheduling changes the number of uplink packets depending on channel condition to maximize system throughput. According to the adaptive control of the number of uplink packets, spatial scheduling has slightly better system throughput than the system without spatial scheduling even under $K = 4$.

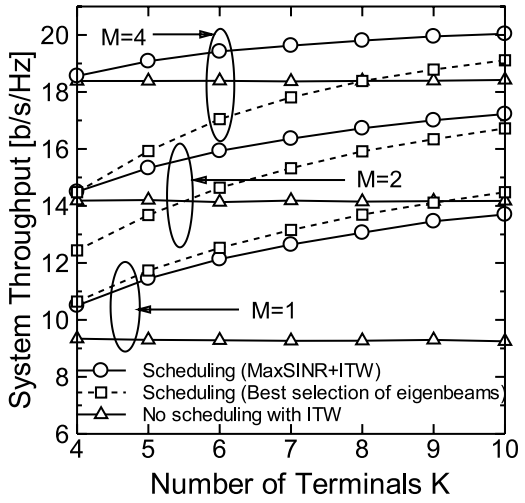

Fig. 5. System throughput of uplink spatial scheduling with iterative transmit weight computation $i_{max} = 3$ under $P_{UL}/P_{BS,z} = 10$ dB.

To examine performance of uplink scheduling algorithm, we compare the maxSINR+ITW algorithm with another algorithm which selects a best combination of terminals' eigenbeams to maximize system throughput. This is achieved by examining system throughputs for all combinations of terminals' eigenbeams, despite the huge complexity. Fig. 5 includes the system throughput of the best combination algorithm of terminals' eigenbeams under $P_{UL}/P_{BS,z} = 10$ dB. In the figure, the maxSINR+ITW algorithm has better performance in $M \geq 2$. This is because terminals perform adaptive transmit beamforming to decrease spatial correlation with other signals at the BS in maxSINR+ITW algorithm whereas terminals do not in the best combination algorithm. The large spatial correlation at the BS results in signal power loss at the BS's receive beamforming. Thus, terminal's transmit beamforming based on system optimization achieves better performance than best combination of terminals' eigenbeams.

Fig. 6 shows the system throughput of uplink spatial scheduling with maxSINR+ITW algorithm versus $P_{UL}/P_{BS,z}$ under 8 terminals ($K = 8$). In the figure, spatial scheduling has large superiority to system without spatial scheduling, specifically under a small number of terminals' antennas M. In smaller M, terminals have severer fluctuation in channel quality and spatial scheduling is more effective in keeping good channel quality of uplink signals. In Fig. 6, the spatial scheduler has at least 2 dB gain under $M \leq 2$.

Fig. 7 shows the system throughput of uplink spatial scheduling without iterative transmit weight (ITW) versus $P_{UL}/P_{BS,z}$ under $K = 8$. Comparing Fig. 6 with Fig. 7, the iterative transmit weight computation has little effect on system throughput of uplink spatial scheduling. It implies that the spatial scheduler keeps good spatial relation of multiplexed signals without iterative transmit weight computation. In contrast, in

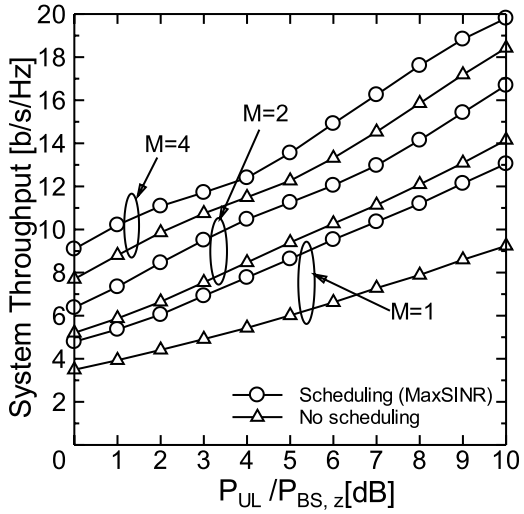

Fig. 6. System throughput of uplink spatial scheduling with iterative transmit weight computation $i_{max} = 3$ under $K = 8$.

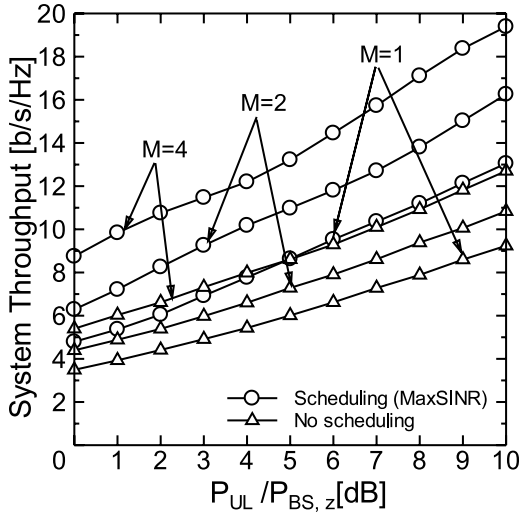

Fig. 7. System throughput of uplink spatial scheduling without iterative transmit weight computation under $K = 8$.

case of no spatial scheduling, system throughput greatly deteriorates without the iterative transmit weight computation. This result shows that the terminals' eigenbeams $\boldsymbol{v}_n^{(0)} = \boldsymbol{e}\langle \boldsymbol{H}_{k(n)}^{*} \boldsymbol{H}_{k(n)}^{T} \rangle$ are not necessarily good in multiuser MIMO system due to the same reason as discussed in Fig. 5.

From these results, we can verify that maxSINR+ITW algorithm is an efficient algorithm for uplink spatial scheduling. In the numerical results, each terminal has fair throughput, because all terminals have the same number of antennas M and the same statistical characteristics of $\boldsymbol{H}_k$. Fair scheduling algorithm under different types of terminals is a subject of future research.

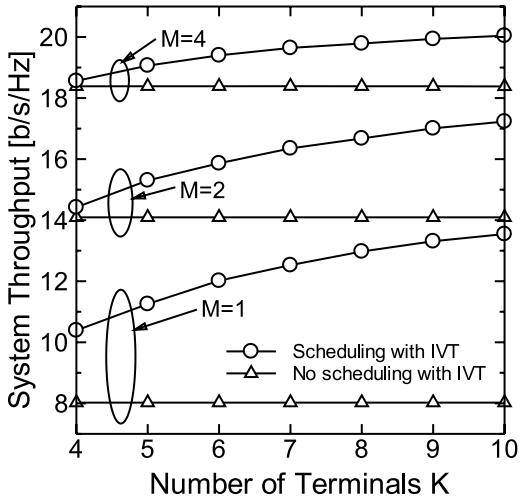

Fig. 8. System throughput of downlink spatial scheduling with iterative virtual weight computation ($i_{max} = 3$) under $P_{DL}/P_z = 10$ dB.

C. System Throughput of Proposed Downlink Spatial Scheduling

Fig. 8 shows the system throughput of the proposed downlink spatial scheduling with iterative virtual weight (IVW) computation under $P_{DL}/P_z = 10$ dB. In the figure, the system throughput is enhanced by the spatial scheduling, because the scheduler can find a better combination of terminals among a larger number of possible terminals. Basically, the system throughput of downlink spatial scheduling is similar to that of uplink scheduling. However, the downlink scheduler has a little worse performance than the uplink scheduler of maxSINR+ITW, because the uplink scheduler uses beamformer of maximizing output SINR whereas the downlink scheduler uses zero-forcing beamformer at the BS. Nevertheless, as K increases, the downlink scheduler finds a good combination of signals with low spatial correlation and the performance difference becomes negligible.

Fig. 9 shows the system throughput of downlink spatial scheduling versus P_{DL}/P_z under 8 terminals ($K = 8$). In the figure, the proposed spatial scheduler has large superiority to the system without spatial scheduling, specifically under small M. Fig. 9 also depicts the system throughput of single-user MIMO system, in which the BS supports only one terminal using multiple eigenbeams with the same transmit power P_{DL}. It is seen that multiuser MIMO system has much higher system throughput than single-user MIMO system.

Fig. 10 shows the system throughput of downlink spatial scheduling without iterative virtual weight computation under $K = 8$. As well as in uplink scheduling, the iterative virtual weight computation has little effect on performance of the proposed spatial scheduling, whereas it has large effect on system

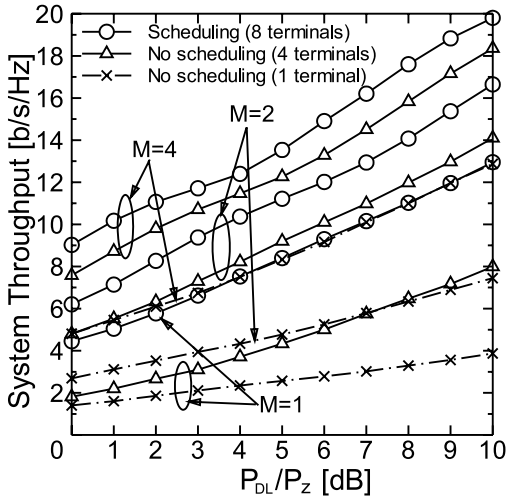

Fig. 9. System throughput of downlink spatial scheduling with iterative virtual weight computation ($i_{max} = 3$) under $K = 8$.

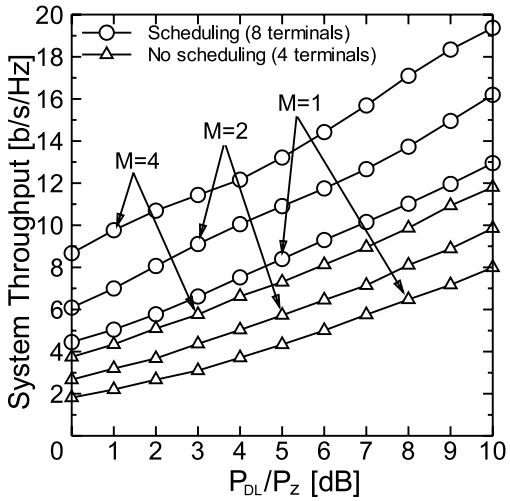

Fig. 10. System throughput of downlink spatial scheduling without iterative virtual weight computation under $K = 8$.

performance in case of no spatial scheduling.

At last, we compare the proposed scheduler with the conventional downlink scheduler : the cooperative zero-forcing with successive encoding with successive allocation method (CZF-SESAM) [17]. In [17], the downlink scheduling algorithm has been optimized, assuming that known interference from previously determined signals can be neutralized by encoding the newly decided signal according to dirty paper coding approach [27]. Performance evaluation has been performed using non-linear or Tomlinson-Harashima precoding as an approximated solution of dirty paper coding.

We consider two cases with and without ideal non-linear precoding in CZF-SESAM. In case of ideal non-linear precoding, inter-stream interference is assumed to be ideally neutralized without any loss of desired signal power, which would give optimistic transmission performance compared to Tomlinson-

Harashima precoding. In case without non-linear precoding, the BS performs only transmit beamforming based on the weight $\check{\boldsymbol{w}}_n$ determined by CZF-CESAM. In general, non-linear precoding requires additional complexity of modulo arithmetics. Using the transmit weights $\check{\boldsymbol{w}}_n$ $(n = 1, ..., N)$ in CZF-CESAM, the BS can predict the received SINR of the n-th signal as

$$\check{\gamma}_{n|n_{DL}} = P_{DL}\check{\boldsymbol{w}}_n^{\dagger}\boldsymbol{H}_{k(n)}^{\dagger}\boldsymbol{R}^{-1}\boldsymbol{H}_{k(n)}\check{\boldsymbol{w}}_n \tag{16}$$

with

$$\boldsymbol{R} = \begin{cases} P_{k(n)z}\boldsymbol{I} & \text{with ideal non-linear precoding} \\ \sum_{l=1,l\neq n}^{n_{DL}} P_{DL}\boldsymbol{H}_{k(n)}\check{\boldsymbol{w}}_l\check{\boldsymbol{w}}_l^{\dagger}\boldsymbol{H}_{k(n)}^{\dagger} + P_{k(n)z}\boldsymbol{I} & \\ & \text{without non-linear precoding} \end{cases}.$$

In case without non-linear precoding, MMSE beamforming is assumed at each terminal. In derivation process of (16), we used relationship of $\check{\boldsymbol{w}}_{l_1}^{\dagger}\check{\boldsymbol{w}}_{l_2} = 0$ $(l_1 \neq l_2)$ in CZF-CESAM. The BS determines MCS of the n-th packet according to the look-up table and the predicted SINR $\check{\gamma}_{n|n_{DL}}$.

Fig. 11 shows the system throughput of the proposed downlink spatial scheduling and CZF-CESAM with ideal non-linear precoding versus number of terminals under $P_{DL}/P_z = 10$ dB. In the figure, CZF-CESAM with ideal non-linear precoding has higher system throughput than the proposed scheduling in $M = 1, 2$, because interference from the other packets is perfectly neutralized without any power loss. Nevertheless, the proposed scheduling has close performance to the CZF-SESAM in case of $M = 4$, because the multiplexed signals have low spatial correlation at the BS and benefit of non-linear precoding becomes small.

To get insight of performance, we evaluate the spatial correlation between multiplexed signals. The spatial correlation is exactly defined as $\langle|\tilde{\boldsymbol{b}}_{n_1}^{\dagger}\tilde{\boldsymbol{b}}_{n_2}|/(||\tilde{\boldsymbol{b}}_{n_1}|| \cdot ||\tilde{\boldsymbol{b}}_{n_2}||)\rangle$ $(n_1 \neq n_2)$, where $\tilde{\boldsymbol{b}}_n = \boldsymbol{H}_{k(n)}^{T}\tilde{\boldsymbol{v}}_n (n = 1, ..., n_{DL})$ and $\langle\cdot\rangle$ denotes the average over all combinations of multiplexed signals. The vector $\tilde{\boldsymbol{b}}_n$ is the response vector of the n-th multiplexed signal at the BS on virtual uplink. Fig. 12 shows the spatial correlation in the proposed scheduling under $P_s/P_z = 0$ or 10 [dB]. Intuitively, the proposed scheduling has drawback in signal power loss caused by different directions of $\tilde{\boldsymbol{b}}_n$ and $\check{\boldsymbol{w}}_n$ in case of high spatial correlation, which results in worse performance than CZF-CESAM with ideal non-linear precoding. As M increases, the spatial correlation decreases thanks to terminal's adaptive beamforming. Accordingly, the proposed scheduling has close system throughput to the CZF-CESAM under large M, due to small power loss at the BS's zero-forcing beamforming. In general, non-linear precoding loses advantage over linear precoding as the spatial correlation decreases. In Fig. 12, the spatial correlation also decreases as

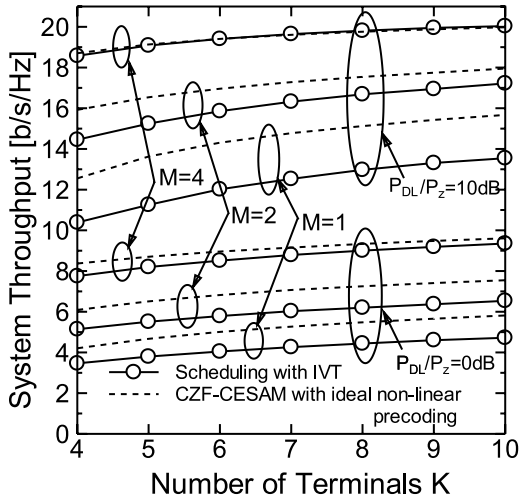

Fig. 11. System throughput of downlink spatial scheduling with iterative virtual weight computation ($i_{max} = 3$) under $P_{DL}/P_z = 10$ dB.

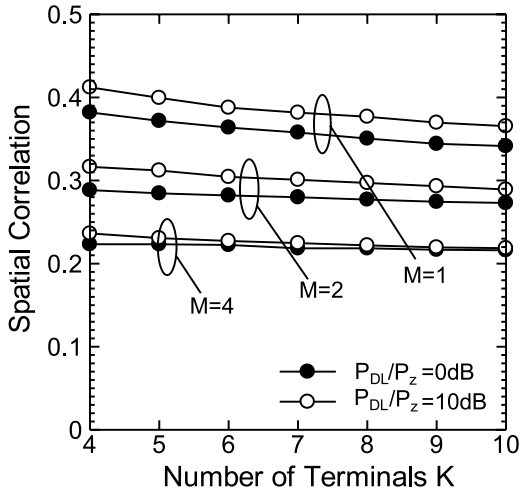

Fig. 12. Spatial correlation versus number of terminals K in downlink spatial scheduling with iterative virtual weight computation ($i_{max} = 3$) under $P_{DL}/P_z = 10$ dB.

K increases from 4 to 10, but the decrease of spatial correlation is not as much as in case of M from 2 to 4. Correspondingly, M from 2 to 4 has more effect on relative performance of the two schedulers than K from 4 to 10 in Fig. 11. Thus, the relative performance of the proposed scheduling and CZF-SESAM with non-linear precoding greatly depends on the spatial correlation.

Fig. 13 shows the system throughput of the proposed downlink scheduling and CZF-SESAM versus P_{DL}/P_z under $K = 8$. As we discussed, CZF-SESAM with ideal non-linear precoding has higher system throughput than the proposed scheduling. However, if the BS uses only linear processing, CZF-SESAM is worse than the proposed downlink scheduling, because terminals are interfered by the other packets in CZF-SESAM. Thus, the proposed scheduler achieves better performance than CZF-SESAM without non-

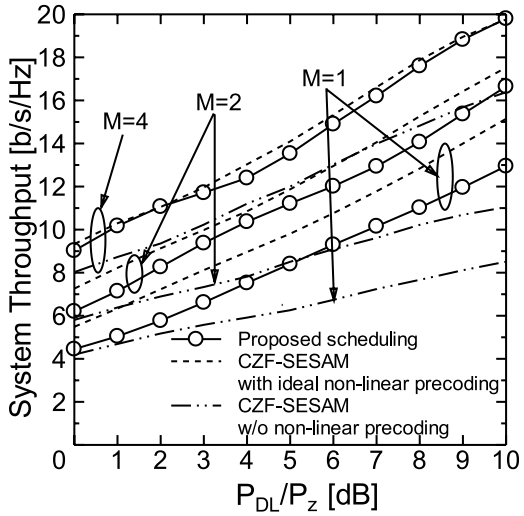

Fig. 13. System throughput of the proposed downlink spatial scheduling with iterative virtual weight computation ($i_{max} = 3$) and CZF-SESAM [17] under $K = 8$.

linear precoding. In reality, whether to use linear or non-linear precoding depends not only on performance and complexity, but also on many aspects, such as total cost of BS, robustness under channel estimation error, system migration scenario, compatibility of legacy terminals, etc. The proposed scheduling is a practical approach to nullify inter-stream interference using linear processing only. From the equivalent property of uplink and downlink scheduling, we can confirm that downlink spatial scheduling has similar system throughput to uplink spatial scheduling.

VI. Conclusion

We proposed downlink spatial scheduling algorithm, which determines an appropriate combination of terminals and transmit beams applying principle of uplink scheduling algorithm. The equivalent property of uplink and downlink scheduling will be useful to apply efficient scheduling algorithm for both uplink and downlink. The numerical results showed that the proposed downlink spatial scheduling achieves much higher system throughput than a multiuser MIMO system without spatial scheduling or with the conventional spatial scheduling by linear processing.

We also presented a basic control structure for uplink and downlink spatial scheduling, which will be a practical scheme in TDD systems. Although we discussed the control structure in isolated cell environment, it would be a prospective future way to apply the control structure in cellular environment, taking into account outer-cell-interference at the BS for uplink scheduling and using the pilot-based CSI feedback [28] for downlink scheduling which represents outer-cell-interference effect of terminals without increasing CSI feedback signalling.

From both aspects of performance and control structure, the presented spatial scheduling is promising towards future wireless communication systems.

APPENDIX I
RECEIVER PERFORMANCE OF INSTRUCTION SIGNALLING

Assume that the BS transmits the n-th instruction signal $\check{s}_n^I(p)$ ($E[|\check{s}_n^I(p)|^2]=1$) for the $k(n)$-th terminal using transmit beamforming weight $\check{\boldsymbol{w}}_n^I$ given by (2). Then, the k-th terminal receives the $M_k \times 1$ signal vector $\boldsymbol{x}_k^I(p)$ as

$$\boldsymbol{x}_k^I(p) \;=\; \sum_{n=1}^{N} \sqrt{P_{DL}^I}\boldsymbol{H}_k \check{\boldsymbol{w}}_n^I \check{s}_n^I(p) + \boldsymbol{z}_k(p) \tag{17}$$

where $E[\boldsymbol{z}_k(p)\boldsymbol{z}_k(p)^\dagger] = P_{kz}\boldsymbol{I}$ and P_{DL}^I is the average transmit power per instruction signal. Note that $(||\check{\boldsymbol{w}}_1^I||^2 + \cdots + ||\check{\boldsymbol{w}}_N^I||^2)/N = 1$ from (2).

If the selected $k(n)$-th terminal computes the target transmit weight $\hat{\boldsymbol{v}}_n$ ($||\hat{\boldsymbol{v}}_n|| = 1$) from responses of the N pilot signals [26], output of the receive beamforming based on the weight $\hat{\boldsymbol{v}}_n$ is given by

$$\begin{aligned}\hat{\boldsymbol{v}}_n^T \boldsymbol{x}_{k(n)}^I(p) &= \hat{\boldsymbol{v}}_n^T \sqrt{P_{DL}^I}\boldsymbol{H}_{k(n)} \check{\boldsymbol{W}}^I \check{\boldsymbol{s}}^I(p) + \hat{\boldsymbol{v}}_n^T \boldsymbol{z}_{k(n)}(p) \\ &= \sqrt{P_{DL}^I}\frac{N^{1/2}||\boldsymbol{H}_{k(n)}^T \hat{\boldsymbol{v}}_n||\check{s}_n^I(p)}{\mathrm{tr}\{(\boldsymbol{B}_{norm}^* \boldsymbol{B}_{norm}^T)^{-1}\}^{1/2}} + \hat{\boldsymbol{v}}_n^T \boldsymbol{z}_{k(n)}(p)\end{aligned} \tag{18}$$

where $\check{\boldsymbol{s}}^I(p) = [\check{s}_1^I(p), ..., \check{s}_N^I(p)]^T$. The $k(n)$-th terminal can receive the n-th instruction nullifying the other instructions using the weight $\hat{\boldsymbol{v}}_n$. The corresponding output SINR is

$$\check{\gamma}_{n|N}^I \;=\; \frac{P_{DL}^I}{P_{kz}} \mu \hat{\boldsymbol{v}}_n^\dagger \boldsymbol{H}_{k(n)}^* \boldsymbol{H}_{k(n)}^T \hat{\boldsymbol{v}}_n \tag{19}$$

$$\geq\; \frac{P_{DL}^I/P_{kz}}{P_{UL}/P_{BS,z}} \mu P_{UL} \hat{\boldsymbol{v}}_n^\dagger \boldsymbol{H}_{k(n)}^* \boldsymbol{\Phi}_{n|n_{UL}}^{-1} \boldsymbol{H}_{k(n)}^T \hat{\boldsymbol{v}}_n \tag{20}$$

with $\mu = N/\mathrm{tr}\{(\boldsymbol{B}_{norm}^* \boldsymbol{B}_{norm}^T)^{-1}\}$. The parameter μ represents power loss due to non-orthogonality among $\boldsymbol{b}_n/||\boldsymbol{b}_n||$ $(n = 1, ..., N)$. In a special case of unitary matrix $\boldsymbol{B}_{norm}$, μ is equal to 1.

In actual wireless systems, control signals can be transmitted with larger power than data signals and $(P_{DL}^I/P_{kz})/(P_{UL}/P_{BS,z})$ in (20) is usually more than 1. Since $P_{UL}\hat{\boldsymbol{v}}_n^\dagger \boldsymbol{H}_{k(n)}^* \boldsymbol{\Phi}_{n|n_{UL}}^{-1} \boldsymbol{H}_{k(n)}^T \hat{\boldsymbol{v}}_n$ in (20), i.e. the output SINR of uplink data signal, is designed properly by uplink scheduler, the selected $k(n)$-th terminal can receive the n-th instruction with good channel quality or small error rate when power loss μ is compensated by the transmit power increase.

APPENDIX II
DERIVATION OF RECEIVED SINR (14)

Given the matrix $\boldsymbol{B} = [\boldsymbol{b}_1, ..., \boldsymbol{b}_n]$ with non-colinear $N \times 1$ vectors $\boldsymbol{b}_1, ..., \boldsymbol{b}_n$ ($n \leq N$), let us consider the $N \times 1$ vector $\boldsymbol{u}_l$ of

$$\begin{aligned} \boldsymbol{u}_l &= \boldsymbol{B}(\boldsymbol{B}^\dagger \boldsymbol{B})^{-1}\boldsymbol{d}_{l|n} = \boldsymbol{b}_l g_l + \bar{\boldsymbol{B}}_{l|n}\bar{\boldsymbol{g}}_l \\ \bar{\boldsymbol{B}}_{l|n} &= [\boldsymbol{b}_1, ..., \boldsymbol{b}_{l-1}, \boldsymbol{b}_{l+1}, ..., \boldsymbol{b}_n] \\ g_l &= \boldsymbol{d}_{l|n}^\dagger (\boldsymbol{B}^\dagger \boldsymbol{B})^{-1}\boldsymbol{d}_{l|n} \\ \bar{\boldsymbol{g}}_l &= [\boldsymbol{d}_{1|n}^\dagger (\boldsymbol{B}^\dagger \boldsymbol{B})^{-1}\boldsymbol{d}_{l|n}, ..., \boldsymbol{d}_{l-1|n}^\dagger (\boldsymbol{B}^\dagger \boldsymbol{B})^{-1}\boldsymbol{d}_{l|n}, \\ &\qquad \boldsymbol{d}_{l+1|n}^\dagger (\boldsymbol{B}^\dagger \boldsymbol{B})^{-1}\boldsymbol{d}_{l|n}, ..., \boldsymbol{d}_{n|n}^\dagger (\boldsymbol{B}^\dagger \boldsymbol{B})^{-1}\boldsymbol{d}_{l|n}]^T \end{aligned} \tag{21}$$

where $\bar{\boldsymbol{g}}_l$ is the $(n-1)\times 1$ vector. From (21), $\boldsymbol{B}^\dagger \boldsymbol{u}_l = \boldsymbol{d}_{l|n}$ holds and is decomposed into $\bar{\boldsymbol{B}}_{l|n}^\dagger \boldsymbol{u}_l = \boldsymbol{0}_{(n-1)\times 1}$ and $\boldsymbol{b}_l^\dagger \boldsymbol{u}_l = 1$. Substituting $\boldsymbol{u}_l$ in (21) into $\bar{\boldsymbol{B}}_{l|n}^\dagger \boldsymbol{u}_l = \boldsymbol{0}_{(n-1)\times 1}$, the vector $\bar{\boldsymbol{g}}_l$ is expressed as

$$\bar{\boldsymbol{g}}_l = -g_l(\bar{\boldsymbol{B}}_{l|n}^\dagger \bar{\boldsymbol{B}}_{l|n})^{-1}\bar{\boldsymbol{B}}_{l|n}^\dagger \boldsymbol{b}_l. \tag{22}$$

Substituting $\bar{\boldsymbol{g}}_l$ into $\boldsymbol{b}_l^\dagger \boldsymbol{u}_l = \boldsymbol{b}_l^\dagger \boldsymbol{b}_l g_l + \boldsymbol{b}_l^\dagger \bar{\boldsymbol{B}}_{l|n}\bar{\boldsymbol{g}}_l = 1$, g_l is represented by

$$g_l = \frac{1}{\boldsymbol{b}_l^\dagger(\boldsymbol{I} - \bar{\boldsymbol{B}}_{l|n}(\bar{\boldsymbol{B}}_{l|n}^\dagger \bar{\boldsymbol{B}}_{l|n})^{-1}\bar{\boldsymbol{B}}_{l|n}^\dagger)\boldsymbol{b}_l}. \tag{23}$$

From (13), the received SINR $\check{\gamma}_{l|n}$ is given by

$$\check{\gamma}_{l|n} = \frac{P_{DL}}{P_{kz}}\boldsymbol{b}_l^\dagger\{\boldsymbol{I} - \bar{\boldsymbol{B}}_{l|n}(\bar{\boldsymbol{B}}_{l|n}^\dagger \bar{\boldsymbol{B}}_{l|n})^{-1}\bar{\boldsymbol{B}}_{l|n}^\dagger\}\boldsymbol{b}_l. \tag{24}$$

APPENDIX III
EQUIVALENCE OF ITERATIVE VIRTUAL WEIGHT COMPUTATION TO ALGORITHM IN [9]

Assume that the $k(l)$-th terminal always receives the l-th packet without spatial scheduling ($l = 1, ..., n_{DL}$). According to [9], conjugate of the $k(l)$-th terminal's receive weight $\tilde{\boldsymbol{v}}_l^*$ is given by the column vector of the left singular matrix of $\boldsymbol{H}_{k(l)}\boldsymbol{Q}_l$ corresponding to the largest singular value. This weight $\tilde{\boldsymbol{v}}_l$ is written in another form as

$$\tilde{\boldsymbol{v}}_l = \boldsymbol{e}\langle \boldsymbol{H}_{k(l)}^* \boldsymbol{Q}_l^* \boldsymbol{Q}_l^T \boldsymbol{H}_{k(l)}^T \rangle \tag{25}$$

where $\boldsymbol{Q}_l$ contains the $N \times 1$ orthogonal basis $\boldsymbol{q}_1$, $\boldsymbol{q}_2$, ... of nullspace against

$$\begin{bmatrix} \tilde{\boldsymbol{v}}_1^T \boldsymbol{H}_{k(1)} \\ \vdots \\ \tilde{\boldsymbol{v}}_{l-1}^T \boldsymbol{H}_{k(l-1)} \\ \tilde{\boldsymbol{v}}_{l+1}^T \boldsymbol{H}_{k(l+1)} \\ \vdots \\ \tilde{\boldsymbol{v}}_n^T \boldsymbol{H}_{k(n)} \end{bmatrix} = \bar{\boldsymbol{B}}_{l|n}^T. \tag{26}$$

Note that $\tilde{\boldsymbol{v}}_l^*$ in [9] may be given by the column vector of the left singular matrix of $\boldsymbol{H}_{k(l)}\boldsymbol{Q}_l$ corresponding to the 2nd largest singular value if two packets are transmitted to the same terminal. However, this weight $\tilde{\boldsymbol{v}}_l$ is still written by (25), because $\boldsymbol{Q}_l$ nullifies the vector $\tilde{\boldsymbol{v}}_{l'}^T\boldsymbol{H}_{k(l')}$ of the other packets to the same terminal.

Since $\boldsymbol{Q}_l^*$ contains orthogonal basis $\boldsymbol{q}_1^*$, $\boldsymbol{q}_2^*$, ... of nullspace against $\bar{\boldsymbol{B}}_{l|n}^\dagger$, we have

$$\boldsymbol{Q}_l^*\boldsymbol{Q}_l^T = \boldsymbol{I} - \bar{\boldsymbol{B}}_{l|n}(\bar{\boldsymbol{B}}_{l|n}^\dagger\bar{\boldsymbol{B}}_{l|n})^{-1}\bar{\boldsymbol{B}}_{l|n}^\dagger. \tag{27}$$

From equivalence of (15) and (25), the iterative virtual weight computation has the same update process of $\tilde{\boldsymbol{v}}_l$ as in [9]. The transmit weight in [9] is the normalized vector of $\boldsymbol{Q}_l\{(\tilde{\boldsymbol{v}}_l^*)^\dagger\ \boldsymbol{H}_{k(l)}\boldsymbol{Q}_l\}^\dagger = (\boldsymbol{Q}_l^*\boldsymbol{Q}_l^T\boldsymbol{H}_{k(l)}^T\tilde{\boldsymbol{v}}_l)^*$. Considering that $\boldsymbol{Q}_l^*\boldsymbol{Q}_l^T\boldsymbol{H}_{k(l)}^T\tilde{\boldsymbol{v}}_l$ is the projection of $\boldsymbol{H}_{k(l)}^T\tilde{\boldsymbol{v}}_l$ on nullspace against $\bar{\boldsymbol{B}}_{l|n}$, the normalized vector of $\boldsymbol{Q}_l^*\boldsymbol{Q}_l^T\boldsymbol{H}_{k(l)}^T\tilde{\boldsymbol{v}}_l$ is equivalent to the normalized vector of $\boldsymbol{B}(\boldsymbol{B}^\dagger\boldsymbol{B})^{-1}\boldsymbol{d}_{l|n}$. Therefore, given the same $\tilde{\boldsymbol{v}}_l$, the transmit weight of (9) corresponds to that in [9]. Thus, in principle, the iterative virtual weight computation algorithm for the fixed terminals is equivalent to the weight computation algorithm in [9].

REFERENCES

[1] E. Telatar, "Capacity of multi-antenna gaussian channels," European Transactions on Telecommunications, vol. 10, no. 6, pp. 585–595, Nov/Dec 1999.

[2] F. R. Farrokhi, G. J. Foschini, A. Lozano, and R. A. Valenzuela, "Link-optimal space-time processing with multiple transmit and receive antennas," IEEE Communications Letters, vol. 5, no. 3, March 2001.

[3] R. L. U. Choi and R. D. Murch, "A transmit pre-processing technique for multiuser MIMO systems: a decomposition approach," IEEE Trans. Wireless Commun., vol. 3, pp. 20–24, Jan. 2004.

[4] K. K. Wong and R. D. Murch, "A joint-channel diagonalization for multiuser MIMO antenna systems," IEEE Trans. on Wireless Commun., vol. 2, pp. 773–786, July 2003.

[5] K. K. Wong, R. S. K. Cheng, K. B. Letaief, and R. D. Murch, "Adaptive antennas at the mobile and base stations in an OFDM/TDMA system," IEEE Trans. on Commun., vol. 49, no. 1, pp. 195–206, Jan. 2001.

[6] S. Serbetli and A. Yener, "Transceiver optimization for multiuser MIMO system," IEEE Trans. on Signal Processing, vol. 52, issue 1, pp. 214–226, Jan. 2004.

[7] Q. H. Spencer, A. L. Swindlehurst, and M. Haardt, "Zero-forcing methods for downlink spatial multiplexing in multiuser MIMO channels," IEEE Transactions on Signal Processing, vol. 52, no. 2, pp. 461–471, Feb. 2004.

[8] A. Bourdoux and N. Khaled, "Joint TX-RX optimisation for MIMO-SDMA based on a null-space constraint," IEEE Proc. of VTC'02 Fall, pp. 171–174, Sept. 2002.

[9] Z. Pan, K. K. Wong, and T. S. Ng, "Generalized multiuser orthogonal space-division multiplexing," IEEE Transactions on Wireless Commun., vol. 3, no. 6, pp. 1969–1973, Nov. 2004.

[10] M. Haardt and A. Alexiou, "WWRF white paper : smart antennas, MIMO systems, and related technologies," WWRF#14-WG4, June, 2005.

[11] Y. J. Zhang and K. B. Letaief, "An efficient resource-allocation scheme for spatial multiuser access in MIMO/OFDM system," IEEE Trans. on Commun., vol. 53, no. 1, pp. 107–116, Jan. 2005.

[12] S. Serbetli and A. Yener "Time slotted multiuser MIMO systems: beamforming and scheduling strategies," EURASIP Journal on Wireless Communications and Networking, issue 2, pp. 286–296, Dec. 2004.

[13] S. Serbetli and A. Yener, "MIMO-CDMA systems: signature and beamformer design with various levels of feedback," IEEE Trans. on Signal Processing, vol. 54, no. 7, pp. 2758–2772, July 2006.

[14] I. Chung, C.S. Hwang, K. Kim, and Y.K. Kim, "A random beamfoming technique in MlMO systems exploiting multiuser diversity," IEEE J. Selected Areas Commun., vol. 21, no. 5, pp. 848–855, June 2003.

[15] M. Sharif and B. Hassibi, "On the capacity of MIMO broadcast channels with partial side information," IEEE Trans. on Information Theory, vol. 51, no. 2, pp. 506–522, Feb. 2005.

[16] Y. Taesang and A. Goldsmith, "Optimality of zero-forcing beamforming with multiuser diversity," IEEE Proc. of ICC2005, pp. 542–546, May 2005.

[17] P. Tejera, W. Utschick, G. Bauch, and J.A. Nossek, "Sum-rate maximizing decomposition approaches for multiuser MIMO-OFDM," Proc. of IEEE PIMRC'05, Sept. 2005.
[18] M. Tomlinson, "New automatic equalizer employing modulo arthimetic," Electronic Letters, vol. 7, pp. 138–139, Mar. 1971.
[19] H. Harashima and H. Miyakawa, "Matched-transmission technique for channels with intersymbol interference," IEEE Trans. on Commun., vol. 20, pp. 774–780, Aug. 1972.
[20] F. R. Farrokhi, K. J. R. Liu, and L. Tassiulas, "Transmit beamforming and power control for cellular wireless systems," IEEE J. Selected Areas Commun., vol. 16, no. 8, pp. 1437–1450, Oct. 1998.
[21] F. R. Farrokhi, L. Tassiulas, and K. J. R. Liu, "Joint optimal power control and beamforming in wireless networks using antenna arrays," IEEE Trans. on Commun., vol. 46, no. 10, pp. 1313–1324, Oct. 1998.
[22] G. Lebrun, T. Ying, and M. Faulkner, "MIMO transmission over a time-varying channel using SVD," IEEE Trans. Wireless Commun., vol. 4, no. 2, pp. 757–764, March 2005.
[23] Wireless World Research Forum (WWRF), "Technologies for the wireless future – section 7," vol. 2 , pp. 227–312, John Wiley & Sons, 2006.
[24] IEEE standard for local and metropolitan area networks Part 16 : air interface for fixed and mobile broadband wireless access systems, in IEEE Std 802.16e, Feb. 2006.
[25] 3GPP RAN, 3G TR 25.814 V1.2.1, "Physical layer aspects for evolved UTRA (Release 7)," Feb. 2006.
[26] Y. Hara and K. Oshima, "Remote control of transmit beamforming in TDD/MIMO system," Proc. of IEEE PIMRC'06, Sept. 2006.
[27] M. Costa, "Writing on Dirty Paper," IEEE Trans. on Inform. Theory, vol. 29, no. 3, pp. 439–441, May 1983.
[28] Y. Hara and K. Oshima, "Pilot-based CSI feedback in TDD/MIMO systems with cochannel interference," Proc. of VTC'06 Fall, Sept. 2006.
[29] Y. Hara, L. Brunel, and K. Oshima, "Uplink spatial scheduling with adaptive transmit beamforming in multiuser MIMO systems," Proc. of IEEE PIMRC'06, Sept. 2006.
[30] Y. Hara, L. Brunel, and K. Oshima, "Downlink spatial scheduling with mutual interference cancellation in multiuser MIMO systems," Proc. of IEEE PIMRC'06, Sept. 2006.

PLACE PHOTO HERE

Yoshitaka Hara received the B. E., M. E., and Dr. Eng. degrees from the University of Tokyo, Tokyo, Japan, in 1993, 1995, and 2003, respectively. In 1996, he joined Mitsubishi Electric Corporation. From April 1999 to December 2001, he was also with YRP Mobile Telecommunications Key Technology Research Laboratories Co., Ltd. From September 2003 to October 2006, he was with Mitsubishi Electric Information Technology Centre Europe B.V. (ITE) in France. Since October 2006, he has been a head researcher at Mitsubishi Electric Corporation, Information Technology R&D Center in Japan. His research interests include wireless transmission schemes and multiantenna techniques. He is a recipient of the Telecom System Technology Award from the Telecommunication Advancement Foundation in 2001 and the IEICE Transactions Best Paper Awards in 2002 and 2006.

PLACE PHOTO HERE

Loïc Brunel (S'97–M'00) was born in Antony, France, in 1973. He received the electrical engineering and Ph.D. degrees from Ecole Nationale Superieure des Telecommunications (ENST), Paris, France, in 1996 and 1999, respectively. Since 2000, he has been a Research Engineer in the Telecommunication Laboratory, Mitsubishi Electric ITE, Rennes, France. His research interests are multicarrier transmissions, code-division multiple access, channel coding, and multiantenna techniques.

PLACE
PHOTO
HERE

Kazuyoshi Oshima was born in Osaka, Japan in 1950. He received the B.S degree from Nagoya Institute of Technology in 1973, the M.S and the Ph.D degrees from the University of Tokyo, in 1975 and 1978, respectively, all in electronics engineering. Since 1978, he has been with Mitsubishi Electric Corporation. He was involved in the research and development of optical fiber transmission system and digital multiplexing equipment. From 1987 to 1988, he was a visiting researcher in University of California, Los Angeles. From 1989, he has been engaged in the research and development of ATM switch LSI, ATM cross-connect system and optical access networks for FTTB/FTTH. From 1997 to 2004, he was engaged in the business development of ATM network systems for telecommunication carrier networks and then in the development of Ethernet based PON system and photonic network system. From October 2004, he has been serving as President of Mitsubishi Electric ITE (Information Technology Center Europe), located in Rennes France and in Guildford UK, and pursuing advanced wireless and optical communication technologies and visual information technologies. Dr. Oshima is a member of the Institute of Image Information and Television Engineers (ITE) of Japan and the IEEE.